ISSN 1070-4272, Russian Journal of Applied Chemistry, 2022, Vol. 95, No. 9, pp. 1418–1426. © Pleiades Publishing, Ltd., 2022.

HYDROGEN TECHNOLOGIES

# An Investigation of the Effect of CuMoB Nanocatalysts on Efficient Hydrogen Production

**Sevilay Demirci[a,*], Mehmet Sait İzgi[b], Hatice Beştaş[b], and Ömer Şahin[c]**

[a] *Department of Chemical Engineering, Faculty of Engineering and Architecture, Kafkas University, Kars, Turkey*
[b] *Department of Chemical Engineering, Faculty of Engineering and Architecture, Siirt University, Siirt, Turkey*
[c] *Department of Chemical Engineering, Istanbul Technical University, Istanbul, Turkey*
**e-mail: incesevilay@gmail.com*

Received November 1, 2022; revised January 16, 2023; accepted January 17, 2023

**Abstract**—In this study, the Cu–Mo–B catalyst in nanostructure was successfully synthesized with the chemical reduction method of sodium borohydride ($NaBH_4$). The categorization of the attained Cu–Mo–B nano-catalyst was examined with XRD, BET, SEM, and EDS analytical methods. As a result of the ammonium borane hydrolysis of this attained catalyst, the most convenient Mo/Co ratio, NaOH impact, the impact of different catalyst amounts, and the impact of different ammonium borane concentrations on ammonium boron hydride hydrolysis were examined. In addition, hydrolysis was examined at different temperatures, and the degree and activation energy of the reaction were determined. At 333 K with the ammonium borane (AB) hydrolysis of Cu–Mo–B nanoparticles, the maximum hydrogen production rate and activation energy were found to be 4075 mL $min^{-1}g_{cat}^{-1}$ and 21.37 kJ $mol^{-1}$, respectively. In this context, Cu–Mo–B catalyst can be used in practical fuel cells since it is obtained economically and easily.

**Keywords:** hydrogen generation, hydrolysis, sodium borohydride, Cu–Mo–B catalyst

**DOI:** 10.1134/S107042722209018X

## INTRODUCTION

The existence of the toxic wastes such as carbon monoxide, carbon dioxide, and unburnt hydrocarbons that spread through the environment after the use of these fuels threatens human health. It is also true that the supply of fossil fuels is limited. One of the most important options among the alternative energy resources that will go beyond the environmental and energy problems in the future is hydrogen energy [1]. Hydrogen is an ideal fuel for proton exchange membrane (PEM) fuel cells in which chemical energy is transformed into electricity energy providing heat and water without the toxic gases that are released to the environment from fossil fuels. However; the greatest problem in using $H_2$ gas as fuel is its low storage efficiency [2–4]. Significant efforts have been made in the development of hydrogen in gas or liquid form stored in pressurized tanks utilizing metal alloys or nanotube-carbon [5, 6]. For this reason, sodium borohydrides with high hydrogen storage capacity have gained great significance as a hydrogen storage environment.

The self-hydrolysis of $NaBH_4$ in alkaline solution is shown as follows:

$$NaBH_4(aq) + 2H_2O \rightarrow 4H_2 + NaBO_2(aq) + \text{heat (217 kJ)}. \quad (1)$$

Reaction [7] occurs when hydrogen production accelerates by conducting alkaline sodium borohydride solution hydrolysis under the conditions generally close to room temperature with the presence of a convenient catalyst. Many metals and compounds have been tested as catalysts for this important reaction. Co–Ni [8–10], Ru [11–13] , Pt [14, 15], Co–B [16–21], Co–Ni–P [22], Pd [23], and Ni–B [24] could be given as examples. However, the noble metal-based hydrogenation catalysts such as Pt, Pd, and Ru are not appealing choices because of their high costs, and this has led to the synthesizing of more economic and more reactive catalysts.

The catalytic hydrolysis of sodium borohydride is also dependent on other parameters such as temperature and the intensity of sodium hydroxide and sodium borohydride as well as the catalyst type. Therefore, researchers have examined the impact of these parameters on the hydrolysis rate of $NaBH_4$ in the presence of various catalysts. For this, there is constant need for cheap and useful catalysts. Cu/Mo atomic ratios were synthesized via the sodium borohydride ($NaBH_4$) reduction method to investigate their performance for ammonia borane hydrolysis.

In this study, first, this prepared catalyst was used to catalyze the hydrolysis of $NH_3BH_3$ ($NH_3BH_3$–HR). The aim was to both increase the catalytic activities of Cu–Mo–B catalysts produced in our country (one of the most important countries of the world in terms of boron reservoirs) and to ensure the production of hydrogen more cheaply by using Cu–Mo–B catalysts in the production of hydrogen from ammonia borane. The structure of the Cu–Mo–B samples were characterized by X-ray diffraction spectroscopy (XRD), Fourier transforms infrared spectroscopy (FTIR), scanning electron microscope (SEM-EDX), and nitrogen adsorption. Furthermore, kinetic parameters such activation energy and reaction order were calculated.

## EXPERIMENTAL

### *Preparation of the Cu–Mo–B Catalyst*

Firstly, the optimum ratio of the $X_{Mo}$=Mo/Cu+Mo (3%) fraction in molar type was determined for borane hydrolysis. For this, first, ammonium molybdenum $(NH_4)_6Mo_7O_{24}$ and copper sulphate ($CuSO_4 \cdot 5H_2O$) were taken in certain amounts, and, after they were mixed in 50 mL water for 15 min, they were in an ultrasonic bath for 30 min for good dispersion of the compounds. After that, they were reduced slowly at 5°C in a nitrogen medium with a 50 mL 2.5% $NaBH_4$ solution. After the attained solution was filtered and washed a few times with pure water and ethyl alcohol, it was dried by leaving it in a drying-oven for 12 h in nitrogen atmosphere at 80°C. The attained Cu–Mo–B catalyst was protected in a closed container for usage purposes in a hydrolysis of ammonium borohydride.

### *Surface Characterization of the Catalyst*

The surface area belonging to the attained catalysts, pore volume, and pore dimension distribution were determined with the Brunauer–Emmett–Teller (BET) surface area. All samples were subjected to a gas removal process (degassing) for 18 h at 423 K before BET analysis.

Also, the surface morphology and crystal structure of the catalyst were respectively determined with SEM (JEOL 6510 scanned electron microscope) and XRD (Cu$K_\alpha$ sourced Rigaku RINT-2000) analyses. The chemical structure of the catalyst and catalyst combinations were explained with EDS (Zeiss EVO 50 Model) analysis.

### *Hydrogen Production*

Ammonium metaborate attained as a result of the hydrolysis of ammonium borane with water and its ratio to hydrogen are dependent on the pH of the solution and particularly temperature. Here, the extension of the half-life of borohydride at certain temperature is generally possible by increasing the pH value. The system here consists of a gas burette, a capped Erlenmeyer flask, and a cryostat with temperature control. The hydrolysis was conducted by adding sodium borohydride solution of a certain amount and concentration to the capped Erlenmeyer flask and by adding the previously prepared catalysts in the ratios of masses determined within the scope of the study. The gas volumes of the synthesized catalysts attained depending on time were collected in the hydrogen gas burette using the prepared water trap. Here, a different NaOH concentration, a different catalyst amount, different $NH_3BH_3$ concentrations, and the volume values of hydrogen gas by considering their efficiency in different temperatures were read at certain periods of time, and the efficiency of the catalyst was graphically determined. According to these attained graphs, data regarding the reaction kinetics such as the activation energy of the reactions and the degree of reaction were obtained.

## RESULTS AND DISCUSSION

### *Characterization and Identification of the Cu–Mo–B Catalyst*

The XRD analysis of the catalysts synthesized in the present study was carried out with the Rigaku RINT-2000 device. The energy dispersive X-ray spectrum and quantitative element analysis results belonging to Cu–B and Cu–Mo–B catalysts can be seen in Fig. 1. In the Cu–Mo–B XRD graph, the $2\theta = 35°$ peak represents Mo(111), $2\theta = 44°$, and 50° sharp peaks show the

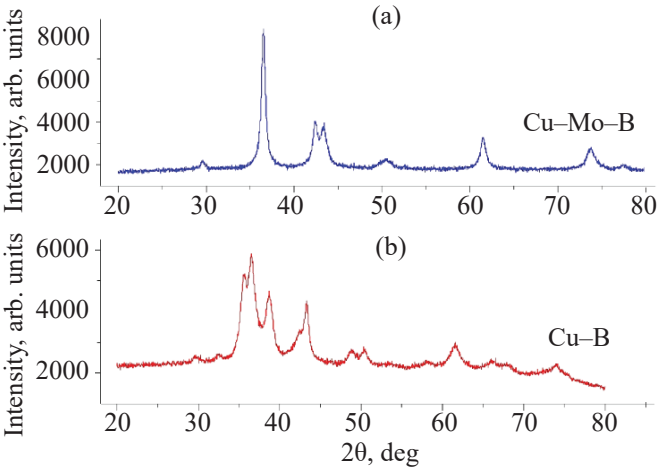


**Fig. 1.** XRD pattern results of Cu–Mo–B and Cu–B.

metallic copper peaks. 2θ = 36.5°, and 43° and the 61° sharp peak show that it is copper oxide [25], and this peak is apparent with the Miller (002) sign. It was observed that there is a 2θ = 45° Cu–Mo–B peak. From XRD graph, it was seen that the desired Cu–Mo–B catalyst was successfully synthesized.

The surface area of the synthesized catalysts was determined with the BET method, and the attained results are given in Table 1. Here, the reason why the surface area of the Cu–B catalyst seems higher than that of Cu–Mo–B catalyst was that the pore structure of the Cu–B catalyst could have a micro structure, and a catalyst (nanocatalyst) with smaller pores was attained by closong the pores by the Mo metal reduced on its surface.

In Fig. 2, SEM analyses were given in the 2k and 10k magnitude ratios for better examination of the surface structure of the Cu–B and Cu–Mo–B catalysts. It may be clearly seen here that significant changes occurred in the surface morphology of the unsupported Cu–Mo–B catalyst with the addition of molybdenum to the Cu–B catalyst. The fact that the spaces in different diameter on Cu–B catalyst surface were filled with the molybdenum addition and smaller pores occurred may also be clearly

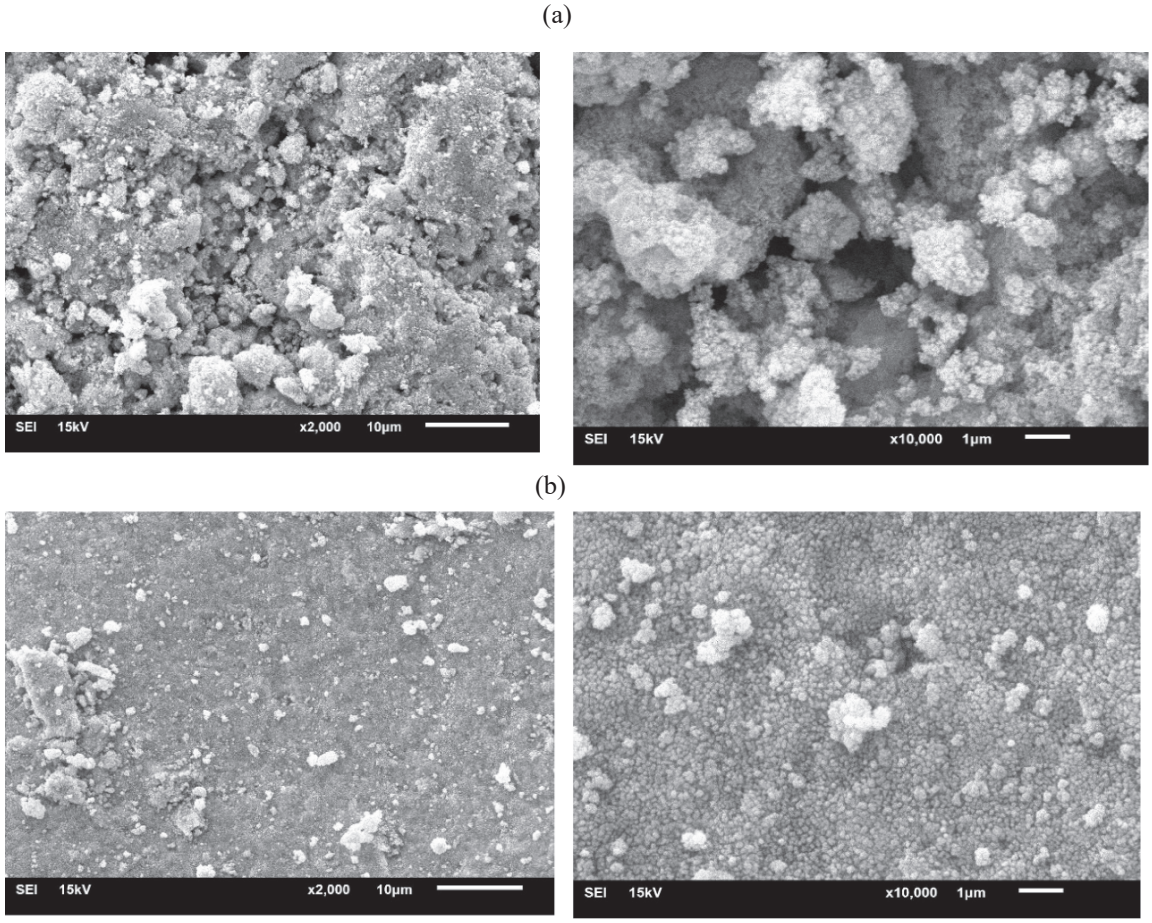


**Fig. 2.** SEM images of (a) Cu–B and (b) Cu–Mo–B catalysts used in ammonium boron hydrolysis in the experimental studies.

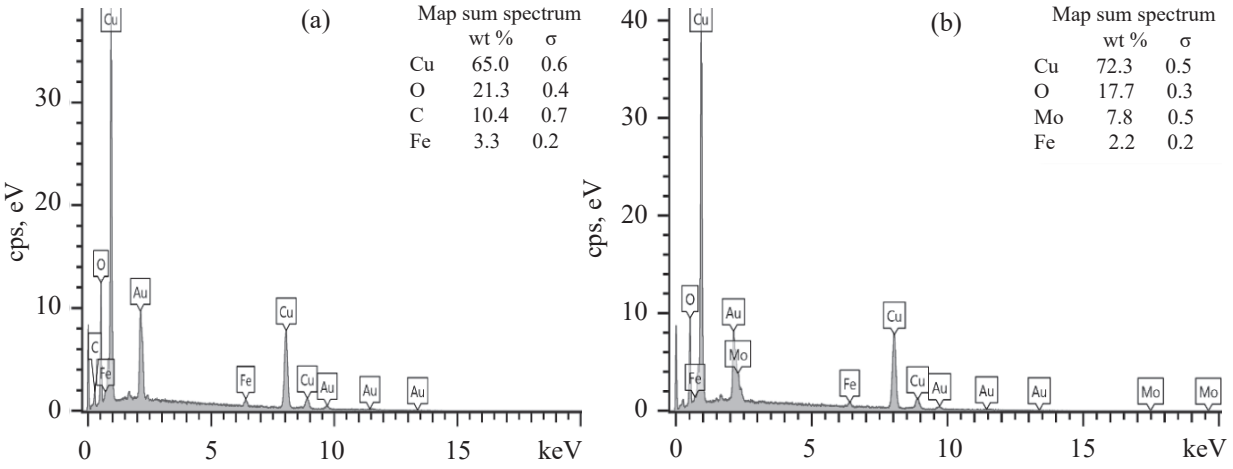


**Fig. 3.** EDS results of (a) Cu–B and (b) Cu–Mo–B.

seen to be supported with the BET results. In other words, it has been observed that the surface of the bimetallic catalyst was smoother, and the catalyst at the nano dimension was attained by loading molybdenum to the Cu–B catalyst, which is not smooth here.

EDX analyses were conducted by scanning an area of 50 μm × 50 μm at a depth of 2.5 μm. When the spectrum given in Fig. 3 is examined, copper (Cu), molybdenum (Mo), oxygen (O), and carbon (C) and their peaks are observed at certain energy zones. The peak belonging to the metal aurum stems from the coating material of the samples coated before the analysis. It was detected from the quantitative element analysis results of the bimetallic Cu–Mo–B catalyst that copper, which is an active metal in the hydrolysis reaction, is existent. Also, it is clearly seen that molybdenum nanoparticles as the second metal have been successfully added to the catalyst structure.

### *Investigation of $NaBH_4$ Hydrolysis Reaction Activity and Kinetics of Cu–Mo–B–Based Catalyst*

$NH_3BH_3$ solution stabilized with 1 wt % NaOH and with 1 mmol water and 10 mL in weight was used as the hydrogen resource in the determination of the optimum molybdenum amount on the supporting surface with high surface area, and activity tests have been conducted at 30°C. The impact of the second metal addition in different concentrations on the performance of copper catalyst was examined. It was determined that the Mo/Cu ratio is 3%. As may be seen from Fig. 4, while the Cu–B catalyst completes the hydrolysis in 30 min, then in the presence of 3% molybdenum the hydrolysis is completed in a shorter period of time (about 5 min).

As it is known, the pH value of the solution is of great importance for hydrolysis. Figure 5 shows the timely change in the hydrogen gas volumes attained as a result of the ammonium borane hydrolysis in the presence of the previously prepared Cu–Mo–B catalyst with addition of NaOH between 1–10 wt % of sodium borohydride solution prepared for this purpose. As seen in Fig. 5, an increase in the catalytic activity of Cu–Mo–B catalyst up to the presence of 2.5% NaOH in the solution medium causes the finalization of the hydrolysis in a longer period of time in the presence of NaOH in higher concentrations. The reason for this result can be explained by the fact that in the 2.5% NaOH solution there are more bases and it is possible that the excess of $OH^-$ anions produced with the increasing NaOH concentration may compete with the transfer of the $BH_4^-$ anion; in this way, the catalyst surface in the system cat be significantly occupied by the $OH^-$ anions coming from NaOH instead of the $BH_4^-$ anions. As a result, the amount of $BH_4^-$ anions in the catalyst surface decreases to produce hydrogen and may cause the decrease in the rate of hydrogen production.

Figure 6 shows the graph of the initial rates vs. NaOH concentrations. As may be seen from the graph,

**Table 1.** BET analysis results of Cu–Mo–B catalyst

| Sample name | Surface area (BET), $m^2/g$ |
|---|---|
| Cu–B | 33.873 |
| Cu–Mo–B | 25.969 |

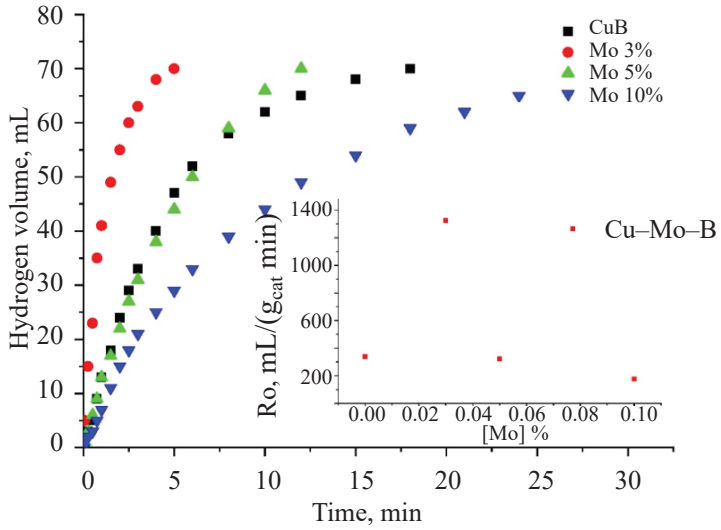


**Fig. 4.** Impact of different metal ratios on hydrogen production speed (30°C, 1 mmol $NH_3BH_3$, 10 mL solution).

while the first value belonging to the hydrolysis is 1500 $H_2/g_{cat}$ min in the presence of 1% NaOH, the rate of hydrogen production in the presence of 2.5% NaOH increases approximately up to 1700 mL $H_2/(g_{cat}$ min), and decreases by 1000 mL $H_2/(g_{cat}$ min) in higher NaOH concentrations.

Another important parameter in the production of hydrogen with the hydrolysis of ammonium borane in the presence of the Cu–Mo–B catalyst is the measurement of the hydrolysis rate depending on the catalyst amount. As seen from the figure, with increasing the catalyst amount at the same concentration, the hydrolysis period also diminishes by the same amount. However, although the hydrolysis period is seen to decrease along with the increase in the catalyst amount, it could be seen from the hydrolysis graph of the initial rate depending on the catalyst amount in the figure that this situation is actually not in direct proportion to the catalyst amount.

As seen from Fig. 7 (inset), while the activity of the catalyst is around 1700 mL $H_2/(g_{cat}$ min) in the presence of the 20 mg catalyst amount, it decreases up to 1100 mL $H_2/(g_{cat}$ min) in the presence of the 30 mg catalyst. The rate of ammonium borane hydrolysis is higher in the presence of 20 mg of catalyst. The possible

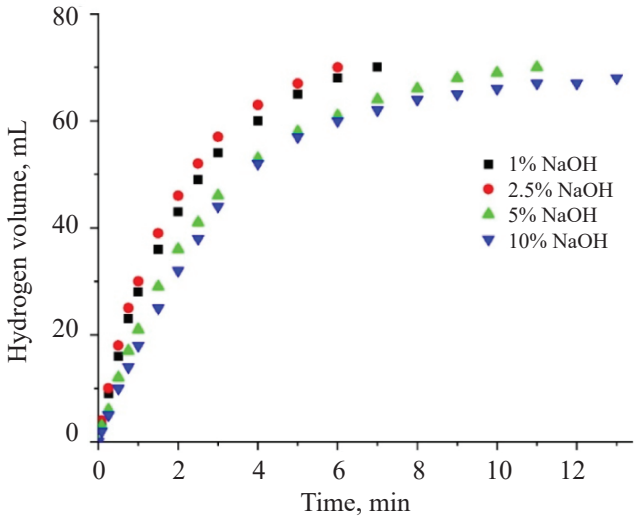


**Fig. 5.** Impact of NaOH concentration on the hydrogen production speed (30°C, 1 mmol $NH_3BH_3$, 20 mg catalyst, 10 mL solution).

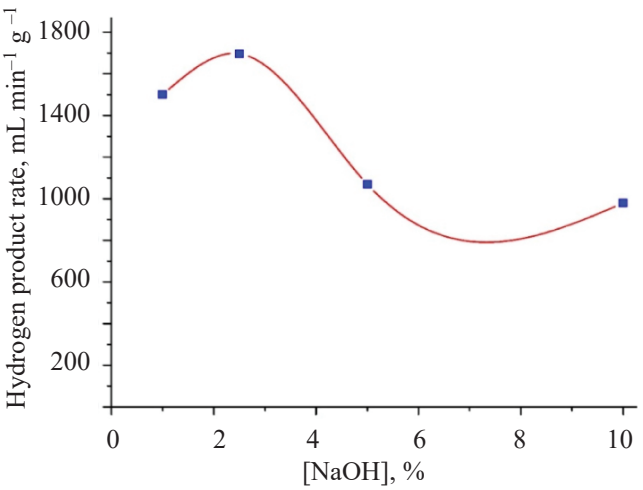


**Fig. 6.** Timely change of the hydrogen volumes in the presence of different NaOH concentrations (1 mmol $NH_3BH_3$, 30°C temperature, 20 mg catalyst, 10 mL solution).

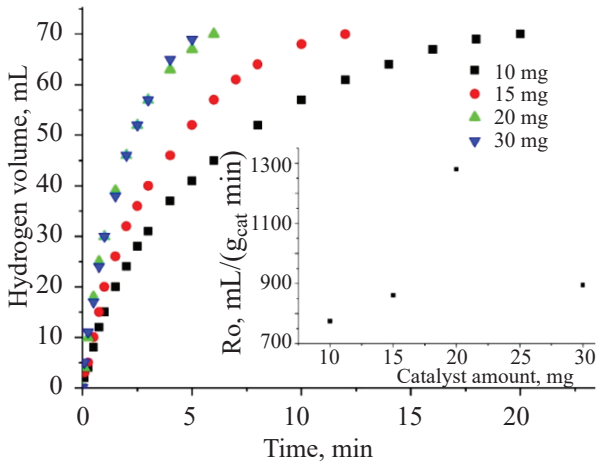


**Fig. 7.** Timely change of the hydrogen volumes attained in AB hydrolysis in the presence of different Cu–Mo–B catalyst amounts (1 mmol $NH_3BH_3$, 30°C temperature, 2.5% NaOH, 10 mL solution).

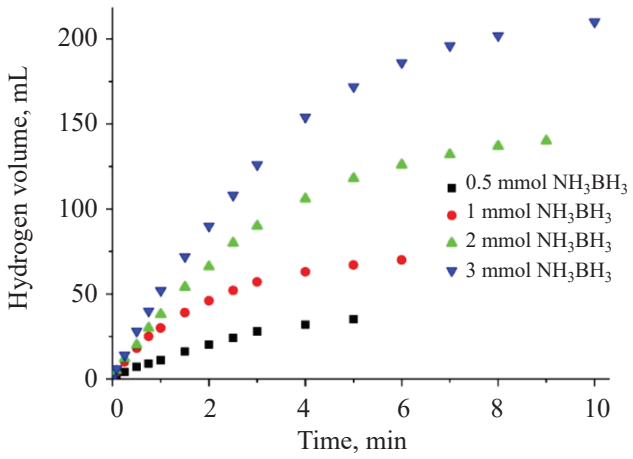


**Fig. 8.** Change in different AB concentrations depending on hydrogen volumes (reaction conditions; 30°C, 20 mg catalyst, 2.5% NaOH, 10 mL solution).

reason for this behavior has been explained by the fact that the active surfaces rise upon increasing the catalyst amount. However, the catalyst goes through many steps to control hydrolysis. The most important of these steps consists of the catalyst control and the diffusion of $BH_4$ anion to the intermediate surface of the solution and afterwards its adsorption to the catalyst surface, the reaction steps, and the desorption of the occurring metaborate. Even if the catalyst surface is increased too much in this situation, it means that the hydrolysis is not only controlled by a single catalyst, but it also controlled by other steps.

As you know, a large amount of fuel for automotive applications is theoretically designed for long-term use. Within this context, the most convenient $NH_3BH_3$ concentration was determined by examining in detail the impact of an $NH_3BH_3$ concentration on the catalytic activity of the Cu–Mo–B catalyst. Experiments were conducted by preparing a solution with (0.5, 1, 2, and 3 mmol) water amounts having different $NH_3BH_3$ concentrations stabilized with 20 mg catalyst and 2.5 wt % NaOH at 30°C.

The graphs in Fig. 8 illustrates situation in which the borohydride concentration in the solution is from 0.5 mmol to 3 mmol, it may seen that the curves of the reactions increase as the concentrations of the reaction substances raise. This behavior is normally totally opposite in most catalysts; namely, the hydrogen output of the viscose structure occurring in the solution is prevented together with the increase in the metaborate concentration in the medium. However, it may be seen here that the hydrogen production rate increases in parallel as the borohydride concentration increases. On the other hand, the change in the initial reaction rates showing the hydrolysis activity with the AB concentration is given in Fig. 9 in the presence of different AB concentrations with the Cu–Mo–B catalyst.

### *Kinetic Studies*

In this study the temperature parameter is important in terms of the calculation of the activation energy for

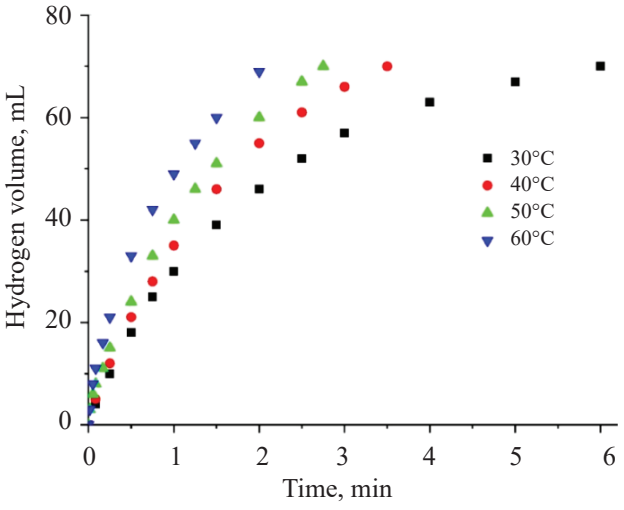


**Fig. 9.** Impact of the reaction temperature on the hydrogen production speed (reaction conditions; 1 mmol AB, 2.5% NaOH, 20 mg catalyst, 30°C, 10 mL solution).

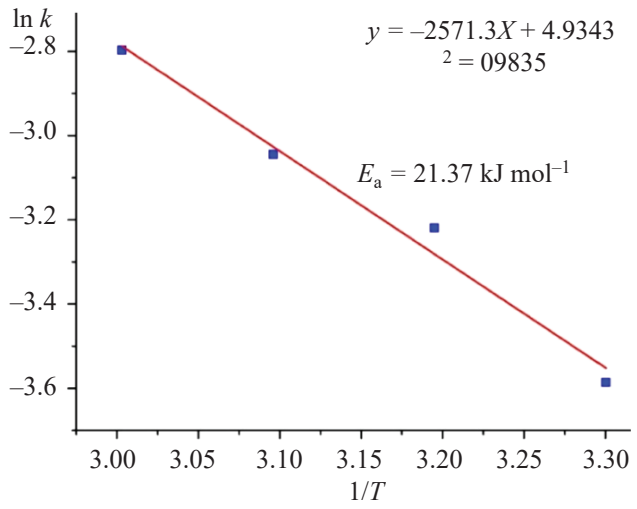


**Fig. 10.** Change of speed constants attained at different temperatures according to the Arrhenius equation.

hydrolysis reaction and also the deduction of the kinetic equation depending on temperature.

Figure 9 demonstrates the temperature ratios of 303, 313, 323, and 333 K. It may be seen that the hydrolysis period also shortens along with the increase in the solution temperature. For instance, while the hydrolysis reaction ends in 6 min at 30°C, the same reaction ends in 2 min at 60°C. The reason for this could be that the increase in the anions and cations along with the increase in temperature (between 30–60°C) and the decrease in the viscosity limits the movements of the ions.

**Table 2.** Comparative statement of reaction results obtained with Cu–Mo–B catalysts and other reported heterogeneous catalysts for the $NaBH_4$ hydrolysis reaction

| Catalyst | Maximum hydrogen product rate mL $min^{-1}$ $g_{cat}^{-1}$ | Activation energy, kJ $mol^{-1}$ | References |
|---|---|---|---|
| Co–Cu–Mo | 1005 | 30.76 | [26] |
| Co–Cu–B | 2120 | 49.6 | [25] |
| Co–Fe–B | 1300 | 31 | [27] |
| Co–Ni–B | 1175 | 34 | [27] |
| Co–B | 875 | 68.87 | [28] |
| Co–Cu–B | 734.4 | – | [29] |
| Cu–B | 1178 | – | [30] |
| Ni–B | 1200 | 58.78 | [31] |
| Cu–Mo–B | 2745 | 21.37 | The current study |

First, the changes of the reaction rate constants with temperature were determined to find the reaction rate constants and activation energy values depending on the temperature and degree of reaction being the kinetic parameters belonging to the AB hydrolysis of the Cu–Mo–B catalyst.

$$-r_{NH_3BH_3}\left(\frac{dC_{NH_3BH_3}}{dt}\right)^n = kC_{NH_3BH_3}, \quad (2)$$

If the integral of Eq. (2) is taken:

$$\ln k = \left[\frac{C_{NH_3BH_3(t=0)}}{C_{NH_3BH_3(t=t)}}\right] = kt. \quad (3)$$

It was determined here that the degree of reaction rate is from the 1st degree. Figure 10 demonstrates the graph of $1/T$ values vs. ln $k$, drawn using the Arrhenius equation:

$$\ln k = \ln A - E_a / RT. \quad (4)$$

As may be seen from Fig. 10; the value of the activation energy of the Cu–Mo–B catalyst belonging to the hydrolysis of sodium borohydride according to the slope of the obtained line is 21.37 kJ/mol. This attained activation energy is too low, and it has significance in terms of showing the valency of the attained catalyst.

Based on the literature data, the comparison of the activation energies and the maximum hydrogen product rate of Cu–Mo-based catalysts is given in Table 2. According to data in Table 2, the activation energy of the 3% Mo : Cu catalyst synthesized in this study is superior compared to others.

As it can be seen from the Table 3, since there is not much difference between the reaction rate constants and

**Table 3.** Comparison of theoretical and experimental in kinetic calculations

| $k$ (exp) | $k$ (theoretical) |
|---|---|
| 0.0277 | 0.03503 |
| 0.04 | 0.033911 |
| 0.0476 | 0.032861 |
| 0.061 | 0.031874 |

Standard deviation for $k$(exp) is 0.012079, $k$(theoretical), 0.001176.

standard deviation obtained at different temperatures; there is little to no experimental error.

## CONCLUSIONS

In this study, the hydrolysis of sodium borohydride was examined in the presence of a Cu–Mo–B catalyst, and the activation energy was determined with kinetic studies. In addition, the surface characterization of the catalyst was examined with advanced analytical methods (BET, SEM, EDX, and XRD).

The most convenient Mo/Cu ratio was determined to be 3 mol %. Our optimum NaOH parameter for the Cu–Mo–B catalyst was determined to be 2.5%. The maximum hydrogen production rate was found to be 2745 mL $min^{-1}$ $g^{-1}$ in 2.5% NaOH and 3 mmol $NH_3BH_3$ concentration at 30°C and was found to be 4075 mL $min^{-1}$ $g^{-1}$ at 60°C. It was determined that the activation energy was 21.37 kJ $mol^{-1}$, and the reaction was from the 1st degree.

The timely change of the hydrogen volumes occurring as a result of the hydrolysis of ammonium borane in the presence of different Cu–Mo–B catalyst amounts is given in Fig. 7 where it may be seen that, as the catalyst amount increases in the same concentration, the hydrolysis period decreases in the same amount. In this study, an easy and cheap synthesis method was developed as a result of the reduction of a multimetallic Cu–Mo–B catalyst with $NaBH_4$.

## ACKNOWLEDGMENTS

The authors would like to acknowledge the Siirt University for their support under the grant number of 2019-SİÜFEN-004.

## CONFLICT OF INTEREST

The authors declare that they have no conflicts of interest.

## REFERENCES

1. İzgi, M.S., *Energy Sources, Part A: Recovery, Utilization, and Environmental Effects,* 2016, vol. 38, pp. 2590–2597.
2. Zhang, J., Fisher, T.S., Gore, J.P., Hazra, D., and Ramachandran, P.V., *International Journal of Hydrogen Energy,* 2006, vol. 31, pp. 2292–2298.
3. Rakap, M. and Özkar, S., *International Journal of Hydrogen Energy*, 2010, vol. 35, pp. 3341–3346.
4. Ma, M., Yang, L., Ouyang, L., Shao, H., and Zhu, M., *Energy*, 2019, vol. 167, pp. 1205–1211.
5. Schlapbach, L. and Züttel, A., *Materials for Sustainable Energy: a Collection of Peer-Reviewed Research and Review Articles from Nature Publishing Group* (World Scientific), 2011, pp. 265–270.
6. İzgi, M.S., Baytar, O., Şahin, Ö., and Kazıcı, H.Ç., *International Journal of Hydrogen Energy*, 2020, vol. 45, pp. 34857–34866.
7. Schlesinger, H.I., Brown, H.C., Finholt, A.E., Gilbreath, J.R., Hoekstra, H.R., and Hyde, E.K., *Journal of the American Chemical Society,* 1953, vol. 75, pp. 215–219.
8. Hua, D., Hanxi, Y., Xinping, A., and Chuansin, C., *International Journal of Hydrogen Energy* 2003, vol. 28, pp. 1095–1100.
9. Şahin, Ö., Kılınç, D., and Saka, C., *Journal of the Energy Institute*, 2016, vol. 89, pp. 617–626.
10. Pornea, A.M., Abebe, M.W., and Kim, H., *Chemical Physics*, 2019, vol. 516, pp. 152–159.
11. Park, J-H., Shakkthivel, P., Kim, H-J., Han, M-K., Jang, J-H., Kim, Y-R., Kim, H-S., and Shul, Y-G., *International Journal of Hydrogen Energy,* 2008, vol. 33, pp. 1845–1852.
12. Liang, Y., Dai, H-B., Ma, L-P., Wang, P., and Cheng, H-M., *International Journal of Hydrogen Energy*, 2010, vol. 35, pp. 3023–3028.
13. Krishnan, P., Yang, T-H., Lee, W-Y., and Kim, C-S., *Journal of Power Sources,* 2005, vol. 143, pp. 17–23.
14. Yin, S-F., Zhang, Q-H., Xu, B-Q., and Zhu, W-X., *Journal of Catalysis,* 2004, vol. 224, pp. 384–396.
15. Patel, N., Patton, B., Zanchetta, C., Fernandes, R., Guella, G., Kale, A., and Miotello, A., *International Journal of Hydrogen Energy,* 2008, vol. 33, pp. 287–292.
16. Xu, D., Dai, P., Liu, X., Cao, C., and Guo, Q., *Journal of Power Sources,* 2008, vol. 182, pp. 616–20.
17. Huang, Y., Wang, Y., Zhao, R., Shen, P.K., and Wei, Z., *International Journal of Hydrogen Energy,* 2008, vol. 33, pp. 7110–7115.
18. Netskina, O.V., Kochubey, D.I., Prosvirin, I.P., Malykhin, S.E., Komova, O.V., Kanazhevskiy, V.V., Chukalkin, Y.G., Bobrovskii, V.I., Kellerman, D.G., and Ishchenko, A.V., *Molecular Catalysis*, 2017, vol. 441, pp. 100–108.
19. Li, F., Li, Q., and Kim, H., *Chemical Engineering Journal,* 2012, vol. 210, pp. 316–424.
20. Shen, X., Wang, Q., Wu, Q., Guo, S., Zhang, Z., Sun, Z., Liu, B., Wang, Z., Zhao, B., and Ding, W., *Energy,* 2015, vol. 90, pp. 464–474.
21. Fernandes, R., Patel, N., and Miotello, A., *Applied*

*Catalysis B: Environmental,* 2009, vol. 92, pp. 68–74.

22. Kim, D-R., Cho, K-W., Choi, Y-I., and Park, C-J., *InternationalJournal of Hydrogen Energy,* 2009, vol. 34, pp. 2622–2630.
23. Kazici, H.Ç., Yildiz, F., İzgi, M.S., Ulaş, B., and Kivrak, H., *International Journal of Hydrogen Energy,* 2019, vol. 44, pp. 10561–10572.
24. Izgi, M.S., Onat, E., Çelik, Kazici, H., and Şahin, Ö., *Energy Sources, Part A: Recovery, Utilization, and Environmental Effects,* 2019, pp. 1–14.
25. Ding, X-L., Yuan, X., Jia, C., and Ma, Z-F., *InternationalJournal of Hydrogen Energy,* 2010, vol. 35, pp. 11077–11084.
26. Deonikar, V.G., Rathod, P.V., Pornea, A.M., Puguan, J.M.C., Park, K., and Kim, H., *Journal of Industrial and Engineering Chemistry,* 2020, vol. 86, pp. 167–177.
27. Patel, N., Fernandes, R., and Miotello, A., *Journal of Catalysis,* 2010, vol. 271, pp. 315–24.
28. Jeong, S.U., Kim, R.K., Cho, E., Kim, H-J., Nam, S-W., Oh, I-H., Hong, S-A., and Kim, S.H., *Journal of Power Sources,* 2005, vol. 144, pp. 129–134.
29. İzgi, M.S., Şahin, Ö., and Saka, C., *International Journal of Hydrogen Energy,* 2016, vol. 41, pp. 1600–8.
30. Figen, A.K., *International Journal of Hydrogen Energy,* 2013, vol. 38, pp. 9186–9197.
31. Ekinci, A., Cengiz, E., Kuncan, M., and Şahin, Ö., *International Journal of Hydrogen Energy,* 2020, vol. 45, pp. 34749–34760.